A functional probe with bowtie aperture and bull's eye structure for nanolithograph*

Wang Shuo(王 硕)[a], Li Xu-Feng(李旭峰)[b]†, Wang Qiao(王 乔)[a], Guo Ying-Yan(郭英楠)[a], and Pan Shi(潘 石)[a]‡

[a] *School of Physics and Optoelectronic Technology, Dalian University of Technology, Dalian* 116024, *China*
[b] *School of Applied Science, Taiyuan University of Science and Technology, Taiyuan* 030024, *China*

(Received 22 February 2012; revised manuscript received 12 June 2012)

The bowtie aperture surrounded by concentric gratings (the bull's eye structure) integrated on the near-field scanning optical microscopy (NSOM) probe (aluminum coated fiber tip) for nanolithography has been investigated using the finite-difference time domain (FDTD) method. By modifying the parameters of the bowtie aperture and the concentric gratings, a maximal field enhancement factor of 391.69 has been achieved, which is 18 times larger than that obtained from the single bowtie aperture. Additionally, the light spot depends on the gap size of the bowtie aperture and can be confined to sub-wavelength. The superiority of the combination of the bowtie aperture and the bull's eye structure is confirmed, and the mechanism for the electric field enhancement in this derived structure is analyzed.

Keywords: surface plasmon polariton, nanolithography, finite difference time domain method

PACS: 73.20.Mf, 42.82.Cr, 02.60.Cb **DOI:** 10.1088/1674-1056/21/10/107302

1. Introduction

The near-field scanning optical microscopy (NSOM)[1] is an efficient method for squeezing light into a nanometer scale region. It has been applied in many applications, including optical storage,[2] nanolithography,[3,4] and single molecule detection.[5] However, according to the classical theory, the transmission efficient scales as $(d/\lambda)^4$,[6] so a serious attenuation occurs when the light transmits through the sub-wavelength aperture. Several approaches have been prompted to enhance the transmission, such as using C-shaped,[7,8] H-shaped,[9] L-shaped,[10] and bowtie-shaped apertures,[11,12] among which the bowtie aperture is the most popular structure due to its larger transmission and higher energy concentration.[13] On the other hand, the sub-wavelength hole arrays have attracted much attention for the enhancement of transmission,[14−16] which is mainly due to the unique properties of the surface plasmon polariton (SPP).[17−19] Meanwhile, a single aperture surrounded by a periodic structure (bull's eye structure) has been proposed to achieve a higher transmission,[20] which also utilizes the propagation of the SPP waves on the metal/dielectric interface. To study the well focusing effect of the bull's eye structure, many experiments and simulations have been carried out.[21−23] As both the bowtie aperture and the bull's eye structure are efficient for enhancing the optical throughput, combining the two structures would be a good choice.[24,25] However, the planar structures limit the application of the scheme on the NSOM due to the poor feedback of the crew-cut probe with given dimensions on controlling the distance between the probe and the sample, so optimizing the scheme on a taper structure is worth studying.

In this paper, we integrate the bowtie aperture with concentric gratings on the aluminum coated fiber probe of NSOM for nanolithography and analyze the enhancement effect of this structure using the finite-difference time domain (FDTD) method. Some parameters of the bowtie and the concentric gratings are modified to optimize the transmission of the light at the wavelength of 365 nm, which is the common working wavelength of photolithography. The best transmission enhancement is 18 times higher than that from the single bowtie aperture without concentric gratings with the same dimension. The mechanism for the electric field enhancement in this derived structure is also studied.

*Project supported by the National Natural Science Foundation of China (Grant Nos. 10974025 and 61137005).
†Corresponding author. E-mail: xfli@mail.dlut.edu.cn
‡Corresponding author. E-mail: span@dlut.edu.cn
© 2012 Chinese Physical Society and IOP Publishing Ltd

2. Method and model

The schematic diagram of a cone structure with a sub-wavelength bowtie aperture surrounded by concentric rings is shown in Fig. 1. The taper fiber tip is covered with an aluminum film containing four concentric rings, and the bowtie aperture is fabricated on the apex of the cone structure. In our calculation, the cone angle φ_1 and the bowtie flare angle φ_2 are set to be 75° and 90°, respectively, and the thickness of the Al film is set to be 100 nm. To optimize the enhancement factor of electric field intensity, we modify the structural parameters, including grating period p, ring width w, gap size g, and outline length a. The frequency-dependent dielectric constant of the aluminum can be characterized by the Drude model

$$\varepsilon(\omega) = \varepsilon_1 + \mathrm{i}\varepsilon_2 = 1 - \frac{\omega_\mathrm{p}^2}{\omega^2+\gamma^2} + \mathrm{i}\frac{\omega_\mathrm{p}^2\gamma^2}{\omega(\omega^2+\gamma^2)}, \quad (1)$$

where $\varepsilon(\omega)$ and ω represent the complex permittivity and the incident light frequency, respectively, the plasma frequency is $\omega_\mathrm{p} = 1.9038\times10^{16}$ rad/s, and the damping rate of the metal is $\gamma = 8.2881\times10^{14}$ rad/s in the visible and ultraviolet region.[26] The FDTD method is employed to calculate the three-dimensional (3D) structure. A 5 nm×5 nm×5 nm mesh is used in the computational domain. The cone structure is illuminated by a plane wave propagating along the $+z$ direction with the polarization along the x direction. Perfect matched layers (PML) are applied for electromagnetic wave absorption.

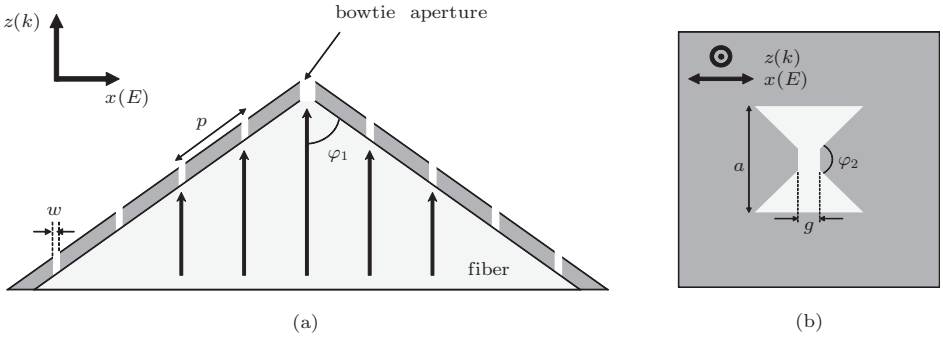


Fig. 1. Schematic diagrams of sub-wavelength bowtie aperture surrounded by concentric rings. (a) Profile view in the x–z plane cut through the middle of the cone structure. (b) Top view of the bowtie aperture.

3. Results and discussion

Due to the momentum mismatch between the SPP waves and the incident light, the SPPs cannot be excited directly by the incident light on the aluminum/fiber interface. The problem can be overcome by fabricating a grating structure on the interface for momentum match, then the condition

$$\beta = k\sin\theta \pm m\cdot 2\pi/p \quad (2)$$

is fulfilled, where k is the wave vector of the incident light in the fiber, θ is the incident angle, m is a positive integer (1, 2, 3, ...), p is the period of the grating, and β is the wave vector of the surface plasmon along the propagating direction. The dispersion of the SPP propagating at the metal/dielectric interface is

$$\beta = k_0\sqrt{\frac{\varepsilon_m\varepsilon_d}{\varepsilon_m+\varepsilon_d}}, \quad (3)$$

where k_0 is the wave vector of the incident light in a vacuum, ε_m and ε_d are the dielectric constants of the aluminum and the fiber, respectively. Period p can be determined from Eqs. (2) and (3) with different incident wavelengths. As the wavelength of the incident light is set to be 365 nm, the dielectric constant of the aluminum can be fixed ($\varepsilon_m = -19.424 + 3.603\mathrm{i}$).[27] Inserting into Eqs. (1) and (2) $k = k_0\cdot n$ and $\varepsilon_d = n^2$, where n is the index of the fiber ($n = 1.52$), $\theta = 90° - \varphi_1$, we obtain the grating period $p \approx 300$ nm.

It is well known that the optical property of a nanostructure strongly depends on the geometry parameters. In order to increase the enhancement factor at the exit of the aperture, the structural parameters should be optimized. The electric field intensity of the x component at the exit of the aperture as a function of the illumination wavelength is shown in Fig. 2 for different ring width w, and the bowtie aperture gap size g and outline length a are set to 50 nm and 150 nm, respectively. It can be found that the main resonant wavelengths almost all appear at 370 nm, which confirms that the grating structure with period $p \approx 300$ nm can concentrate the illumi-

nation (λ = 365 nm) at the apex of the taper fiber; the result is in good agreement with Wang's work.[28] In the result, the resonant peak increases gradually when the ring width decreases from 70 nm to 30 nm, and the maximum enhancement factor of the electric intensity is about 68 at the ring width of 30 nm. As the aluminum film is completely cut off by the air rings, the SPP waves excited by the illumination light have to transmit through the separated aluminum film to the apex of the fiber. As the SPP waves cross a ring, opposite charges will be introduced on the edges of the ring, providing a quasi-electrostatic coupling across the ring. Therefore, the phase change will be sensitive to the ring width. It can be found that as the main peak decreases, pits start to appear at the main peak (Fig. 2, w = 60 nm, w = 70 nm), which suggests that further increasing the ring width leads to the momentum mismatch between the SPP waves and the incident light. However, as the ring width is much smaller than the SPP wavelength, the concentric rings will have little effect on the excitation of the SPP wave, and the phase change will be very small.[29]

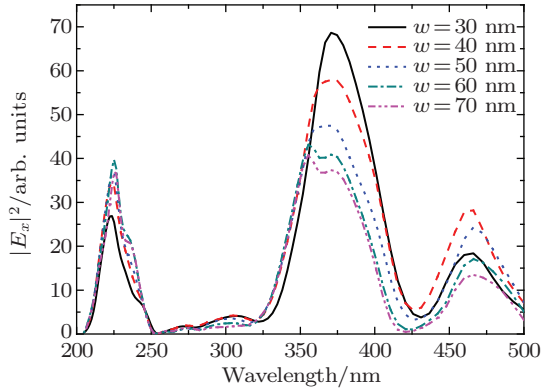


Fig. 2. (colour online) Electric field intensities of the x component (E_x) as a function of incident wavelength for different ring widths.

As the bowtie structure influences the transmission of light, the bowtie apertures with different gap sizes are studied, and the results are shown in Fig. 3. The bowtie aperture outline length is kept the same (a = 150 nm), and the ring width is set to the optimized value 30 nm. Clearly, with the gap size decreased from 70 nm to 30 nm, the enhancement factor increases dramatically, and the maximum electric field intensity is about 178 times higher than the intensity of the incident light (achieved at g = 30 nm). As the charge tends to accumulate at the two tips of the bowtie aperture, the electric field intensity will be enhanced in the gap area. As the gap size decreases, the electric field coupling between the two tips will become stronger, which further increases the charge density in the two tips. Therefore, the dipole-like radiation will be enhanced when the gap size is reduced. Additionally, the resonant wavelength is still at 370 nm, and no obvious change is found with the different gap sizes.

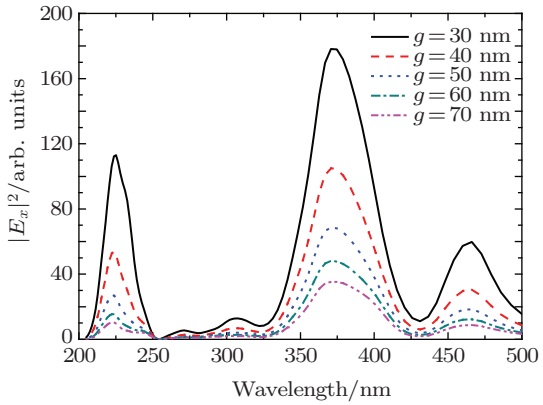


Fig. 3. (colour online) Electric field intensities of the x component (E_x) as a function of incident wavelength for different gap sizes.

Based on the above results, the outline length a is modified to achieve a higher enhancement, the calculation result is shown in Fig. 4, where the ring width and the gap size are all set to be 30 nm. It can be found that the resonant wavelength shows a red shift with the outline length increasing, which is well consistent with the other works.[30,31] Especially, the maximal electric field intensity, which is about 391.69 times higher than the intensity of the incident light, is obtained at the exit of the aperture with the outline length of a = 90 nm. Moreover, the resonant wavelength is 365 nm, which is the working wavelength of photolithography.

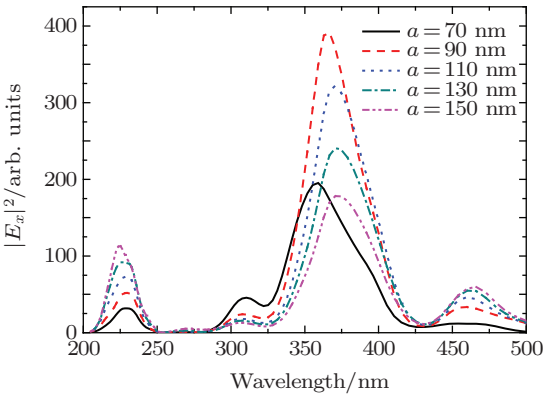


Fig. 4. (colour online) Electric field intensities of the x component (E_x) as a function of incident wavelength for different outline lengths.

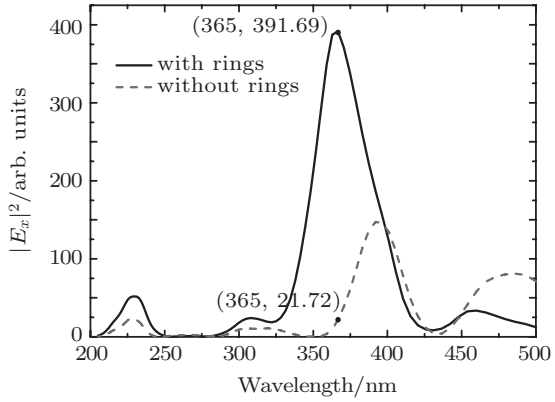


Fig. 5. Electric field intensities of the x component (E_x) as a function of incident wavelength. The solid line shows the bowtie aperture with concentric rings (ring width $w = 30$ nm), and the dash line shows the bowtie aperture without concentric rings. The parameters of the bowtie apertures are the same, $g = 30$ nm and $a = 90$ nm.

It should be noticed that as the wavelength of the incident light is 365 nm, the bowtie aperture with the dimension outline length $a = 90$ nm and gap size $g = 30$ nm does have an obvious enhancement effect on the light in the fiber directly illuminating the aperture. However, as more light propagates through the aluminum/fiber interface with concentric rings to the apex in the form of SPP waves, the total electric field intensity is greatly increased at the apex. For comparison, the bowtie aperture ($a = 90$ nm and $g = 30$ nm) without concentric rings is studied (Fig. 5). It shows that the resonant wavelength of the single bowtie structure is 392 nm and the enhancement factor is about 147. When the wavelength of the incident light is selected to be 365 nm, the enhancement factor is just 21.72, which is 18 times smaller than that obtained from the bowtie with grating structure. The distributions of electric field intensity (wavelength $\lambda = 365$ nm) in the x–y plane at the exit of the bowtie aperture with and without the grating structure are illustrated in Fig. 6. The light transmitting to the apex through the bull's eye structure is further enhanced by the bowtie aperture. Moreover, it is clear that the energy is concentrated to the gap and the spot size is mainly determined by the gap scale. A higher intensity sub-wavelength light spot can be obtained from this scheme. However, owing to the limit of the cone structure dimension and the specified working wavelength (365 nm), the enhancement effect of the bowtie aperture is not fully demonstrated. Changing the period of the concentric rings and choosing the wavelength of light source at the resonant wavelength of the bowtie aperture can further increase the enhancement effect of the bowtie aperture.

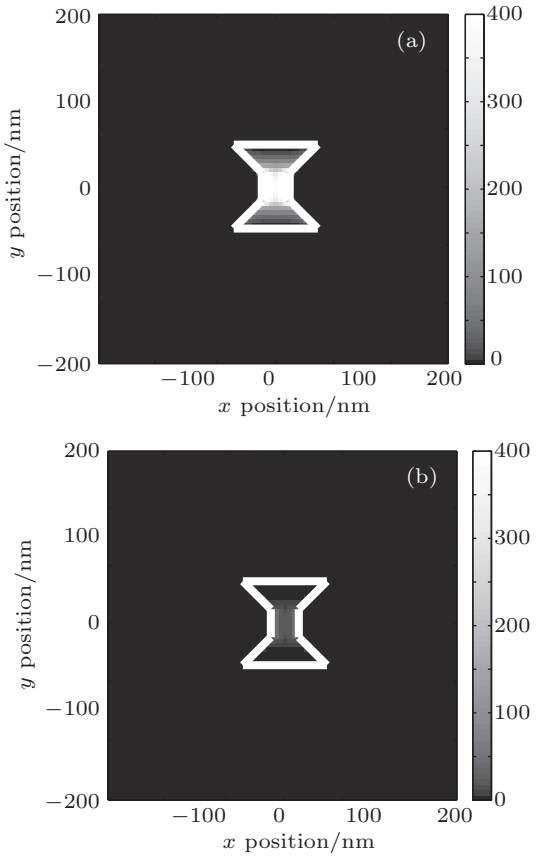


Fig. 6. Distributions of electric field intensity (wavelength $\lambda = 365$ nm) in the x–y plane at the exits of the bowtie apertures (a) with (ring width $w = 30$ nm) and (b) without grating structure, where $g = 30$ nm and $a = 90$ nm.

4. Conclusion

In summary, the bowtie aperture and the bull's eye structure have been efficiently combined for transmission enhancement of the NSOM probe. By modifying the structure parameters, a maximal field enhancement factor of 391.69 is achieved at 365 nm (the common working wavelength of photolithography) in our calculation. In our model, the main mechanism for the electric field enhancement is that the incident light is concentrated to the apex of the fiber cone by the bull's eye structure and further enhanced by the bowtie aperture. The single bowtie aperture without the concentric grating structure has also been calculated for comparison; its enhancement factor is only 21.72, which further confirms the advantage of our derived structure. Moreover, the light spot can be confined to sub-wavelength and is mainly determined by the gap size of the bowtie aperture. Such a combination with a much higher enhancement factor provides

an efficient and promising method for nanolithography.

References

[1] Betzig E, Lewis A, Harootunian A, Isaacson M and Kratschmer E 1986 *Biophys. J.* **49** 269

[2] Betzig E, Trautman J, Wolfe R, Gyorgy E, Finn P, Kryder M and Chang C H 1992 *Appl. Phys. Lett.* **61** 142

[3] Smolyaninov I I, Mazzoni D L and Davis C C 1995 *Appl. Phys. Lett.* **67** 3859

[4] Herndon M, Collins R, Hollingsworth R, Larson P and Johnson M 1999 *Appl. Phys. Lett.* **74** 141

[5] Betzig E and Chichester R J 1993 *Science* **262** 1422

[6] Bethe H 1944 *Phys. Rev.* **66** 163

[7] Shi X, Hesselink L and Thornton R L 2003 *Opt. Lett.* **28** 1320

[8] Matteo J, Fromm D, Yuen Y, Schuck P, Moerner W and Hesselink L 2004 *Appl. Phys. Lett.* **85** 648

[9] Jin E and Xu X 2007 *J. Heat Transfer* **129** 37

[10] Xu J Y, Wang J, Gai H F, Tian Q, Wang B X, Hao Z B and Han S 2006 *Chin. Phys. Lett.* **23** 2587

[11] Şndur K and Challener W 2003 *J. Microsc.* **210** 279

[12] Wang L, Uppuluri S M, Jin E X and Xu X 2006 *Nano Lett.* **6** 361

[13] Jin E X and Xu X 2005 *Appl. Phys. Lett.* **86** 111106

[14] Ebbesen T W, Lezec H, Ghaemi H, Thio T and Wolff P 1998 *Nature* **391** 667

[15] Martin-Moreno L, Garcia-Vidal F, Lezec H, Pellerin K, Thio T, Pendry J and Ebbesen T 2001 *Phys. Rev. Lett.* **86** 1114

[16] Sun M, Liu R J, Li Z Y, Cheng B Y, Zhang D Z, Yang H F and Jin A Z 2006 *Chin. Phys.* **15** 1591

[17] Raether H 1988 *Surface Plasmons* (Berlin: Springer-Verlag)

[18] Zhou F, Liu Y and Li Z Y 2011 *Chin. Phys.* B **20** 037303

[19] Liu B C, Yu L and Lu Z X 2011 *Chin. Phys.* B **20** 037302

[20] Lezec H, Degiron A, Devaux E, Linke R, Martin-Moreno L, Garcia-Vidal F and Ebbesen T 2002 *Science* **297** 820

[21] Lockyear M J, Hibbins A P, Roy Sambles J and Lawrence C R 2005 *J. Opt.* A: *Pure Appl. Opt.* **7** S152

[22] Mahboub O, Palacios S C, Genet C, Garcia-Vidal F, Rodrigo S G, Martin-Moreno L and Ebbesen T 2010 *Opt. Express* **18** 11292

[23] Carretero-Palacios S, Mahboub O, Garcia-Vidal F, Martin-Moreno L, Rodrigo S G, Genet C and Ebbesen T 2011 *Opt. Express* **19** 10429

[24] Ishihara K, Ohashi K, Ikari T, Minamide H, Yokoyama H, Shikata J and Ito H 2006 *Appl. Phys. Lett.* **89** 201120

[25] Kinzel E C, Srisungsitthisunti P, Li Y, Raman A and Xu X 2010 *Appl. Phys. Lett.* **96** 211116

[26] Markovic M I and Rakic A D 1990 *Appl. Opt.* **29** 3479

[27] Lide D R 2004 *CRC Handbook of Chemistry and Physics: A Ready-Reference Book of Chemical and Physical Data* (Boca Raton: CRC Press)

[28] Wang Y, Sriturayanich W, Sun C and Zhang X 2008 *Nano Lett.* **8** 3041

[29] Steele J M, Liu Z, Wang Y and Zhang X 2006 *Opt. Express* **14** 5664

[30] Wang L and Xu X 2007 *Appl. Phys.* A: *Mater. Sci. & Process.* **89** 293

[31] Guo H, Meyrath T P, Zentgraf T, Liu N, Fu L, Schweizer H and Giessen H 2008 *Opt. Express* **16** 7756